

# BioNTech RNA-Based COVID-19 Injections Contain Large Amounts Of Residual DNA Including An SV40 Promoter/Enhancer Sequence

Link: <https://publichealthpolicyjournal.com/biontech-rna-based-covid-19-injections-contain-large-amounts-of-residual-dna-including-an-sv40-promoter-enhancer-sequence/#abstract>

ULRIKE KÄMMERER VERENA SCHULZ KLAUS STEGER \*

PEER REVIEWED, CLINICAL RESEARCH

12/03/2024

[v5.2019-2024](#)

## Abstract

---

**Background:** BNT162b2 RNA-based COVID-19 injections are specified to transfect human cells to efficiently produce spike proteins for an immune response.

**Methods:** We analyzed four German BNT162b2 lots applying HEK293 cell culture, immunohistochemistry, ELISA, PCR, and mass spectrometry.

**Results:** We demonstrate successful transfection of nucleoside-modified mRNA (modRNA) biologicals into HEK293 cells and show robust levels of spike proteins over several days of cell culture. Secretion into cell supernatants occurred predominantly via extracellular vesicles enriched for exosome markers. We further analyzed RNA and DNA contents of these vials and identified large amounts of DNA after RNase A digestion in all lots with concentrations ranging from 32.7 ng to 43.4 ng per clinical dose. This far exceeds the maximal acceptable concentration of 10 ng per clinical dose that has been set by international regulatory authorities. Gene analyses with selected PCR primer pairs proved that residual DNA represents not only fragments of the DNA matrices coding for the spike gene, but of all genes from the plasmid including the SV40 promoter/enhancer and the antibiotic resistance gene.

**Conclusion:** Our results raise grave concerns regarding the safety of the BNT162b2 vaccine and call for an immediate halt of all RNA biologicals unless these concerns can be dispelled.

## Keywords

[BNT162b2](#), [cell transfection](#), [Comirnaty](#), [COVID-19](#), [plasmid](#), [RNA-vaccine](#), [SV40 promoter/enhancer](#)

## Introduction

---

In 2020, politically promoted campaigns like “Operation Warp Speed” [1,2] and “Project Lightspeed” [3,4] pushed the development of a completely new class of drugs finally aiming at vaccinating seven billion people worldwide against COVID-19 [5]. These so-called “mRNA-vaccines” – hereinafter referred to as RNA injections or RNA biologicals –

consist of nucleoside-modified mRNA (modRNA) packaged in transfection-competent lipid nanoparticles (LNP). According to the underlying idea, modRNA, once in the cell, forces this cell to produce SARS-CoV-2 spike proteins and present it on the cell surface, subsequently resulting in the stimulation of the immune system to generate specific antibodies against the presented spike antigen [6,7]. The “speed of science” [8] and the demand of the governments worldwide faced the manufacturers with the challenge to produce large amounts of modRNA within a very short time. Thus, the initial PCR-based process for the generation of the DNA matrices (process-1) for modRNA production, which received authorization for use in the phase-3 clinical trial, very soon reached its limits and the companies switched to a large-scale production of DNA matrices via cloned shuttle vectors, which can be easily multiplied in bacterial cell culture systems (process-2) [9]. Starting with the governmental vaccine roll-out, this process-2 product was employed instead of the original product.

Already in 2021, it has been reported that the modRNA-induced spike proteins could be found circulating in the blood of vaccinees weeks after the injections [10]. In 2022, the first detailed post-mortem investigation revealed the presence of vaccine-induced spike proteins at multiple locations in vessel walls and different tissues weeks after the last BNT162b2 injection [11]. Recently, vaccine-induced spike proteins were identified in placentas of women injected with RNA biologicals during pregnancy [12]. Dhuli and colleagues reported the presence of a sequence corresponding to a fragment of the modRNA in blood cells of long-COVID patients with a history of two doses of the BioNTech/Pfizer vaccine [13]. Importantly, the production of spike proteins by the body cells is not restricted to the injection area and did not terminate within a few days as had been proclaimed by the manufacturers and the responsible authorities. Several mechanisms have been suggested so far that could contribute to the remarkable long-lasting expression of spike proteins in vaccinated individuals.

First, biologicals contain nucleoside-modified mRNA (modRNA) to extend its lifetime [14], to reduce its destruction by turning off toll-like receptor detection [15], and to maximize its translation. This was achieved by replacing natural uridines with synthetic N1-methylpseudouridines (mPsi) and by increasing the content in guanine and cytosine (known as codon optimization) [6,14,16].

Second, transfected modRNA may be reverse transcribed into DNA and integrated into the cell’s genome via a LINE1 (Long Interspersed Nuclear Element-1) mediated mechanism, as data from transfection experiments in human cell lines HEK293T [17] and Huh7 [18] suggested.

Third, lipid nanoparticles (LNP) delivering modRNA to the cells may also contain DNA, which originated from the production process, where spike-coding DNA was used as a template for the in-vitro transcription of modRNA. Remaining DNA may not completely be separated from modRNA and degraded by deoxyribonuclease-I (DNase-I) digestion and, subsequently, be packaged in the LNP together with the modRNA. It is well known that DNase-I can adhere to the surfaces of reaction vessels and can exhibit reduced efficiency in the presence of hybrids of DNA and RNA [19]. According to a manufacturer, it is “probably impossible to remove every single strand of DNA in an RNA preparation” [20]. Given the fact that the European Medicines Agency and the German Paul Ehrlich Institute fixed a residual DNA of 10 ng per injected clinical dose as acceptable (and indeed DNA

up to this margin was shown in the registration documents [9]), it makes a packaging of this DNA into the lipid nanoparticles highly likely.

This possibility emerged on the scene in February 2023, when McKernan and colleagues announced the discovery of large amounts of both spike-coding DNA and residual plasmid-DNA derived from the expression vector system in BioNTech/Pfizer and Moderna vaccine lots [21,22]. The bulk was represented by fragmented, linearized DNA, but also intact plasmids being able to successfully transfect *E. coli* cells [21,22]. Assuming that these intact plasmids were packaged in the LNP together with the modRNA, stable expression vectors could enter the cells and thus provide a rich source of long-lasting spike production in the case that the cells are able to transcribe the coded spike region. Incomprehensibly, plasmids from BioNTech/Pfizer, but not from Moderna, do not only contain the bacterial T7 promoter system, but also the mammalian Simian Virus 40 (SV40) promoter/enhancer sequence [23-25]. This gives cause for concern, as already in 1999, Dean and colleagues demonstrated that nuclear entry of plasmid-DNA, especially in non-dividing cells, requires a 72 bp sequence of the SV40 promoter/enhancer [23]. Of note, neither the promoter, nor the origin of replication are needed for nuclear localization of plasmid-DNA [23]. Meanwhile, the results of the McKernan team have been confirmed and extended [26]. Recently, König and Kirchner published data on large amounts of residual DNA within several BNT162b2 lots [27].

Against this background, we performed a series of experiments to answer the following urgent questions. First, can the large amount of residual DNA in BioNTech lots [27] and even plasmids identified in Pfizer lots [21,22] be confirmed on BioNTech only lots (BNT162b2, Comirnaty) distributed in Germany by different comparable DNA detection methods? Second, can residual plasmids or DNA fragments, if present, be efficiently transfected into human cells together with the coding modRNA? Third, can these biologicals induce continued cellular expression of spike protein thus creating long-term foci for immune attack? To answer these questions, we applied an in-vitro cell culture model using HEK293 cells, as these cells simulate dividing human cells and, therefore, are not only a suitable target for protein production but are also most susceptible for a potential interaction of the transfected foreign nucleic acids and the cell's genome. The fact that we obtained positive results on all issues raises the strongest concerns on the safety of the BNT162b2 vaccine.

## **Materials and Methods**

---

### ***Vaccine Lots***

The following original and unopened BNT162b2 vaccine lots were used: FD7958 (monovalent Wuhan; expiry date October 2021), FE6975 (monovalent Wuhan; expiry date October 2021), EX8679 (monovalent Wuhan; expiry date August 2021), HD9869 (bivalent Wuhan/Omicron XBB1.5; expiry date October 2024). As positive control for the PCR reaction and mass spectrometry analysis, lot GH9715 (bivalent Wuhan/Omicron BA.4 and BA.5; expiry date June 2023) was used, because its contamination with the SV40 containing plasmid was proven already [25]. The vials were provided to us by the pharmacy in the manufacturer's refrigerated state. They were unopened and always refrigerated during transport and storage.

### ***Cell Line Experiments and ELISA***

HEK293 cells were grown in a humidified incubator at 37 °C, 5% CO<sub>2</sub>. The cells used were from original stocks (Cell Lines Service GmbH, Eppenheim, Germany) regularly tested negative for mycoplasma and stored in aliquots in liquid nitrogen. Cells were thawed fresh prior to transfection experiments, cultured in 10 cm well dishes with DMEM with 10% fetal calf serum supplemented with 1% penicillin/streptomycin until confluency and transferred after trypsinization (0.05% trypsin/EDTA (Gibco #11500636; 3 min 37 °C) to new wells, according to the experimental set up described below.

For all transfection experiments, the vials with the monovalent mRNA were pre-diluted 1:5 with sterile RNase-free phosphate-buffered saline (PBS) to the clinical concentration, according to the manufacturer. The bivalent vials were not pre-diluted since the clinical concentration was already present. For ELISA, 12-well plates with 80% cell density and a medium volume of 1 ml each were transfected with 1/12 (25 µl) of a clinical dose of a vial and cells and media were harvested at time points day 1, day 3, day 5, and day 7. Untransfected cells at day 7 served as negative control. For protein analysis, cells were washed twice in sterile phosphate-buffered saline (PBS) after the respective incubation time (see above), lysed in lysis buffer (25 mM Tris, 150 mM NaCl, 1% Triton-X-100, 1% NP40, pH 7.6) and the spike protein level was determined in the protein supernatant and the media using a commercially available high-sensitive S-Plex SARS-CoV-2 Spike ELISA assay (Mesoscale Discovery K150ADJS).

### ***Immunohistochemistry***

Immunohistochemistry was performed using a standard protocol. In brief, 60% dense cells on 24-well plates were transfected with 12.5 ml of a clinical dose per well in 200 ml medium. After 4h of incubation, the cells were washed twice with sterile PBS and 500 ml fresh growing media were applied to the wells. 24h after the start of transfection, cells were harvested, fixed in 4% buffered paraformaldehyde, embedded in 2% agarose/water and dehydrated using a standard dehydration protocol for biopsy samples. Thereafter, the agarose blocks were embedded in paraffin and cut. Sections were placed on Superfrost slides, dewaxed twice with xylene and rehydrated in a graded series of ethanol and in distilled water. After rehydration and antigen retrieval (ACD biotechne #322000, 15 min steamer), the slides were permeabilized (0.3% Triton-X-100/PBST), treated with peroxide suppressor (Thermo Scientific #35000), and blocked in PBS with 1% goat serum, 1% BSA, 0.1% Triton-X-100, and 0.05% Tween-20. Then, the slides were incubated with the rabbit polyclonal antibody against SARS-CoV-2 spike protein (S1-subunit) (ProSci #9083) overnight at 4 °C, washed in PBS, and incubated with anti-rabbit poly-HRP antibody (Invitrogen #32260) for 30 min at room temperature. Protein detection was performed using permanent HRP Green Kit (Zytomed), counterstained in hematoxylin, and embedded in RotiHistol II Kit.

### ***DNA and RNA Quantification***

One clinical dose of each vial was diluted 1:10 with sterile RNase-free PBS supplemented with 1% Triton-X-100. For quantification of RNA, 10 µl of the diluted clinical dose was applied on a black 96-well plate in triplicates and treated with Qubit RNA High Sensitivity Assay (Invitrogen #Q32852). For quantification of dsDNA, 10 µl of the diluted clinical dose was applied on a black 96-well plate in triplicates and treated with Qubit dsDNA High Sensitivity Assay (Invitrogen #Q33230), Quanti-iT Pico Green dsDNA Assay (Invitrogen #P7589), or AccuBlue High Sensitivity dsDNA Assay (Biotium #31006-T). RNase A (final concentration 50 µg/ml, DNase-free Monarch RNase A #T3018L) treatment was performed at 37 °C for 30 min. Signals of all assays were quantified with a standard plate reader at excitation 483 nm and emission 530 nm. There was no signal overlap between

excitation and emission wavelengths for the respective fluorophores used in the kits. We measured the amount of DNA and RNA (Figure 1 A-C) and calculated the DNA/RNA ratio relative to 1 mg RNA. These ratios were put in relation to the EMA regulation of 0.33 mg dsDNA per 1 mg RNA. From this, we obtained the increase factor in Table 3 and Figure 1D.

### ***Polymerase Chain Reaction (PCR)***

To isolate plasmid DNA from cells, 6 cm dishes with cells at 80% density were transfected with half of a clinical dose of each vial (150 ml /well) added to 1ml of medium.

Untransfected cells served as negative control. After 6h, cells were harvested, washed twice in PBS, and plasmid DNA was purified (Gene Jet Plasmid Mini Kit). Aliquots of 1-10 ng DNA were loaded into each PCR reaction.

To determine the DNA content in the vials, one clinical dose of each vial was diluted 1:10 in EB buffer (10 mM Tris-HCl, pH 8.5) supplemented with 1% Triton-X-100. For the PCR reaction, primers were designed using PrimerBlast and ordered via Eurofins Genomics, dissolved in nuclease-free water and used as final concentration of 0.2 mM. For the location of the primer pairs in relation to the expression vector, see Figure 3A. 1 µl of the diluted solution was used as template and processed according to standard Taq polymerase protocol (94 °C 30 sec, 60 °C 30 sec, 72 °C, 30 sec, 38 cycles) using Taq DNA polymerase with Standard Taq Buffer (New England Biolabs #M0273S). Nuclease-free water served as negative control. A vial containing batch GH9715 was used as a positive control, as plasmid DNA from this batch was already isolated and sequenced [21,22] and confirmed to refer to the plasmid sequence BNT162b2 (GenBank PP544445.1, GenBank PP544446.1, GenBank MQ287666.1 representing sequence 16 from patent WO2021214204) published by BioNTech. The isolated and previously sequenced plasmid from lot GH9715 served as positive control. The primers applied are described in Table 1. Finally, the PCR reactions were loaded onto a 2% agarose gel with ethidium bromide in standard TAE buffer (running time ~ 1h; 100V). Gene Ruler DNA-Ladder Mix (Thermo Scientific #SM0331) was used as DNA marker.

Sequence name	Forward primer (5' - 3')	Reverse primer (5' - 3')	Amplicon (bp)
spike protein aa24-98	CCTACACCAACAGCTTTACC	GATGTTGGACTTCTCGGTGC	221
spike protein aa258-328	CGCTTACTATGTGGGCTACC	TGGTGATATTGGGGAACCGC	212
spike protein aa534-654	GAACTTCAACTTCAACGGCC	AGCTATTGTTACGTGCTCG	362
spike protein aa1183-1269	GGTGGCCAAGAATCTGAACG	CATGTGTAGTGCAGTTTCACG	258
ORI	CTACATACCTCGCTAATC	GCGCCTTATCCGGTAACTATC	150
neomycin cassette	GACCACCAAGCGAAACATCG	CCACCATGATATTCGGCAAGC	195
SV40 promoter/enhancer	CCAGCTGTGGAATGTGTGTC	GCTGACTAATTGAGATGCATGC	93+165

**Table 1.**

Characterization of the primers used for PCR.

### ***EV Isolation and Secretome Concentration***

Cells were grown in 6 cm dishes to 80% density and transfected with half of a clinical dose (150  $\mu$ l) of the bivalent lot GH9750 added to 1 ml of medium. Untransfected cells served as negative control. After 6h, cells were washed and media was changed to 5 ml fresh media. After further 18h, media were collected and cells were washed twice in PBS, harvested and further processed for mass spectrometry.

EV isolation was performed as previously reported using the Vn-96 peptide capture method that precipitates EVs via binding to HSPs at the EV surface [28,29]. In brief, 20  $\mu$ l of the VN-96 peptide (Microvesicle Enrichment kit, New England Peptide, #W1073-2, USA) was added to the cell conditioned medium (2 ml) obtained from HEK293 (un)transfected cells, and incubated on a rotation wheel for 1h at room temperature. EVs were isolated after centrifugation for 15 min at 16,000 xg at 4 °C. The supernatant (soluble secretome) was collected into a new tube and concentrated using a 3kDa MWCO filter (Merck, Amsterdam, The Netherlands, cat. no. UFC500396). EV pellet was washed once with 1 ml PBS (4 °C) containing PIC (complete Mini EDTA-free, #11836153001 Roche, Germany).

### ***Sample Preparation For Proteomics***

Sample preparation for proteomics was performed as previously described [30,31]. To this end, an aliquot of the cell pellet suspension in PBS, corresponding to ~25 mg of protein was lysed in 30 ml LDS sample buffer (containing 10% dithiothreitol, Life Technologies, Carlsbad, CA, cat. no. NP0008), 20 ml soluble secretome was lysed with 10 ml 3x LDS sample buffer, and EV pellet was solubilized in 30  $\mu$ l 1x LDS sample buffer, all at room temperature. Subsequently, samples were heated for 5 min at 99 °C and sonicated (3x 20 sec) and fractionated using gel electrophoresis in precast Bis-Tris 4-12% gradient gels using the NuPAGE SDS-PAGE system (Invitrogen, Carlsbad, CA) at room temperature. Following electrophoresis, gels were fixed in 50% ethanol / 3% phosphoric acid (Merck, Switzerland) solution and stained overnight with Coomassie Brilliant Blue R-250 (Thermo Scientific, UK) at room temperature. Subsequently, the gels were washed with 25 ml 50 mM ammonium bicarbonate (Fluka, Seelze, Germany) and with 25 ml 50 mM ammonium bicarbonate with 50% acetonitrile (Biosolve BV, Valkenswaard, The Netherlands). Proteins were reduced and alkylated by incubating the whole gel in 25 ml dithiothreitol for 1h at 56 °C and 25 ml 55 mM iodoacetamide (Sigma-Aldrich, USA) for 45 min at room temperature, respectively. Gel lanes were cut into 3 bands and each band was cut into ~1 mm<sup>3</sup> cubes. The gel cubes from each band were dried in a SpeedVac centrifugal evaporator for 10 min at 50 °C and incubated ~100-200 ml (enough to cover) with 6.25 ng/ml sequencing grade modified trypsin (Promega, Madison, USA) overnight at room temperature. The peptides from each gel band were extracted with 100-150 ml 1% formic acid and two times with 100-150 ml 5% formic acid / 50% acetonitrile, lyophilized and stored at -20 °C until LC-MS/MS analysis.

### ***Mass Spectrometry-Based Proteomics***

Label-free proteomics of lysates, EV, and soluble secretome samples was performed using an Evosep chromatography system coupled to a TimsTOF-HT MS/MS system (Bruker, Germany). Peptides (600 ng / sample as determined by Nanodrop) were dissolved in 0.1% FA and loaded on Evotips (Evosep, Denmark) as per manufacturer protocol. Peptides were separated via nanoflow reversed-phase liquid chromatography using standardized gradients on an Evosep One liquid chromatography system (Evosep, Denmark) with 0.1% FA and 0.1% FA / 99.9% ACN as the mobile phases at room temperature. The 30 samples per day (SPD) method was used in combination with a 15 cm x 150  $\mu$ m reverse-phase column packed with 1.5  $\mu$ m C18-beads (Bruker Daltonics) connected to a 20  $\mu$ m ID fused silica emitter (Bruker Daltonics). Peptides were introduced to a TimsTOF HT (Bruker Daltonics) using a nano-electrospray ion source (Captive spray

source, Bruker Daltonics) with spray voltage set to 1500 V. The TimsTOF HT was running in DDA-PASEF mode with a ramp time set to 100 ms and ten PASEF scans were acquired per topN acquisition cycle, resulting in a cycle time of 1.16 s. Precursors with a mass range from 100 m/z to 1700 m/z, ion mobility range from 1.5 to 0.7 Vs cm<sup>-2</sup>, and charge states from 0 (unassigned) to 5+ were analyzed. The intensity threshold was set to 2,500 arbitrary units (a.u.) and target value to 20,000 a.u. Precursors that reached this target value or full scheduling capacity were excluded for 0.4 min. Single charged precursors were filtered out based on their m/z-ion mobility position. Precursors with a mass below 700 Da were isolated with a quadrupole isolation width of 2 Th, precursors above 700 Da with a width of 3 Th. Collision energy was linearly decreased from 59 eV at 1.6 Vs cm<sup>-2</sup> to 20 eV at 0.6 Vs cm<sup>-2</sup>. For all experiments, the ion mobility dimension was calibrated linearly using three selected ions of the Agilent ESI LC/MS Tuning Mix [m/z, 1/K0: (322.0481, 0.7318 Vs cm<sup>-2</sup>), (622.0289, 0.9848 Vs cm<sup>-2</sup>), (922.0097, 1.1895 Vs cm<sup>-2</sup>)].

MS/MS spectra were searched using MaxQuant 2.3.1.0 against the reviewed human proteome (Uniprot, March 2023, 42420 entries including isoforms) and the sequences of the Moderna mRNA1273 expression vector, Pfizer bivalent expression vector BNT162b2 and the severe acute respiratory syndrome coronavirus 2 isolate Wuhan-Hu-1 spike protein sequence, plus their ribosomally frameshifted translation products. Enzyme specificity was set to trypsin, and up to two missed cleavages were allowed. Cysteine carbamidomethylation (Cys, +57.021464 Da) was treated as fixed modification, and methionine oxidation (Met, +15.994915 Da) and N-terminal acetylation (N-terminal, +42.010565 Da) as variable modifications. Peptide and protein identifications were filtered at an FDR of 1% using the decoy database strategy. The minimal peptide length was 7 amino acids. Proteins that could not be differentiated based on MS/MS spectra alone were grouped into protein groups (default MaxQuant settings). Searches were performed with the label-free quantification option selected. Proteins were quantified by spectral counting [32].

## Results

---

### ***Successful Transfection Of Cells Results In The Production of Spike Protein***

The modRNA-containing lipid nanoparticles represent a powerful tool for the transfection of mammalian cells [33]. To test for transfection effectiveness, we analyzed the expression pattern of spike proteins after transfecting human embryonic kidney cells (HEK293) with four different BioNTech (Comirnaty) vaccine lots, namely the monovalent lots FD7958, FE6975, EX8679, and the bivalent lot HD9869. All four lots successfully transfected the HEK293 cells, as demonstrated by a strong spike protein immunohistochemical signal (Figure 1A). The transfection efficiency as rated by spike-positive cells was 90.5%, 74.6%, 76.4%, 80.7%, and 0% for lots FD7958, FE6975, EX8679, HD9869 and untreated cells, respectively. In addition, transfected cells showed clear signs of a cytopathic effect compared to the non-transfected (control) cell line, as evidenced by the formation of large vacuoles and detached cells (Figure 1B). To quantify the spike protein expression stability over time, we measured the amount of spike protein in cell lysates after 1, 3, 5, and 7 days using a commercially available ELISA. All four lots followed the same expression pattern with already clear expression of spike protein after day 1, increasing production until day 5, and still higher spike concentration on day 7 than on day 1 (Figure 1C).

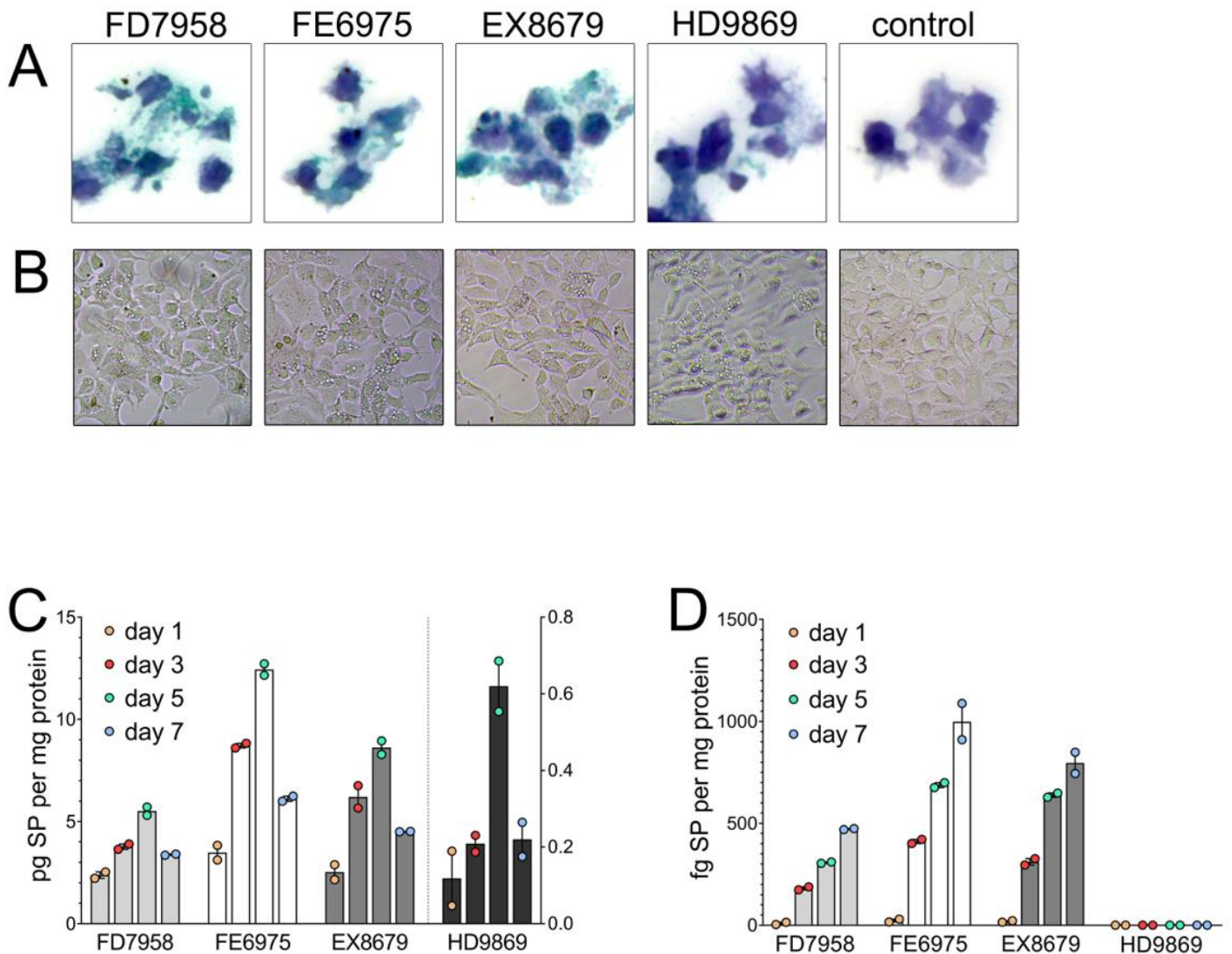


**Figure 1.**

Spike protein expression in HEK293 cells after transfection with BNT162b2 biologicals. A: Staining of spike proteins in cells transfected with different lots visualized in green color by immunohistochemistry. Non-transfected cells (control) show no staining. Hematoxylin serves as nuclei counterstain. B: Brightfield microscopy of transfected HEK293 cells with different lots show an accumulation of intracellular vesicle formation. C: Quantification of intracellular spike protein (SP) concentrations over time measured by ELISA. n=2; mean+SEM. D: Quantification of secreted spike protein (SP) levels over time measured by ELISA. For lot HD9869, secreted spike protein concentration was below the detection limit. n=2; mean+SEM. The negative control showed no spike protein content in the cell lysate and cell supernatant. SEM, standard error of the mean.

### ***Spike Protein Is Released Into The Supernatant Of Transfected Cell***

To determine whether spike proteins are presented on the cells only or can either shed off or be secreted from the transfected cells, we analyzed the cell-free culture supernatant for spike proteins applying ELISA. The measured values are cumulative quantities from day 0 to the respective indicated time point. We observed a clear increase in the amount of spike protein in the media over time in the three monovalent lots. The spike protein concentration in the media of cells transfected with the bivalent lot HD9869 was below the ELISA detection limit (Figure 1D).

### ***Spike Protein Is Mainly Released Via Extracellular Vesicles***

The luminal part of membrane proteins can be cleaved at the membrane surface by different cellular secretases and released into the medium, but uncleaved proteins can

also be secreted from the cells via extracellular vesicles (exosomes). We used mass spectrometry to clarify by which mechanism spike proteins were secreted into the supernatant after artificial transfection of the cell line with the lot GH9715 as model system. To this end, both the transfected cells and the medium were harvested after 24h of transfection. As a result of the isolation of the extracellular vesicles (EV) from the medium, we gained three fractions – the cell lysate, the EVs, and the EV-free medium for proteome profiling. The results of the spike protein abundance in the three fractions are presented in Table 2. The spike protein was most abundant in the lysate (60 spectral counts) and clearly present in the EVs (14 spectral counts), while only low levels (2 spectral counts) were found in the EV-free medium. Importantly, control transfected cells were negative for spike protein and, as expected, common EV markers (CD81, TSG101, alix) were enriched in the EV fraction versus the soluble secretome and detected in both transfected and untransfected cells.

	Spike protein		Extracellular vesicle markers					
	Control	BioNTech	CD81		TSG101		Alix	
			Control	BioNTech	Control	BioNTech	Control	BioNTech
Cellular lysate	0	60	18	23	3	5	38	61
Extracellular vesicles	0	14	14	18	7	6	51	36
Soluble secretome	0	2	1	3	0	0	0	1

**Table 2.**

Number of spectral counts (protein abundance) in specific fractions of the HEK293 cell line transfected with the bivalent BioNTech vial GH9715.

***RNA Concentration Of The Tested Vials Corresponds To The Declaration Of BioNTech***

To confirm the quality of the lots used in the transfection reactions, we tested the RNA content of the vials by Qubit RNA High Sensitivity Assay. Results confirmed that the vials contained the amount of RNA declared by the manufacturer as 30 µg RNA per clinical dose (Figure 2A). Performing triplicate analysis, the RNA content of lot FD7958 was found to be 26.74 + 0.31 (mean + SEM) µg RNA per estimated clinical dose, lot FE6975 contained 28.57 + 0.22 µg RNA, lot EX8679 26.51 + 0.59 µg RNA, and lot HD9869 28.12 + 0.47 µg RNA per clinical dose, demonstrating the high reliability of the handling and nucleic acid quantification method used herein.

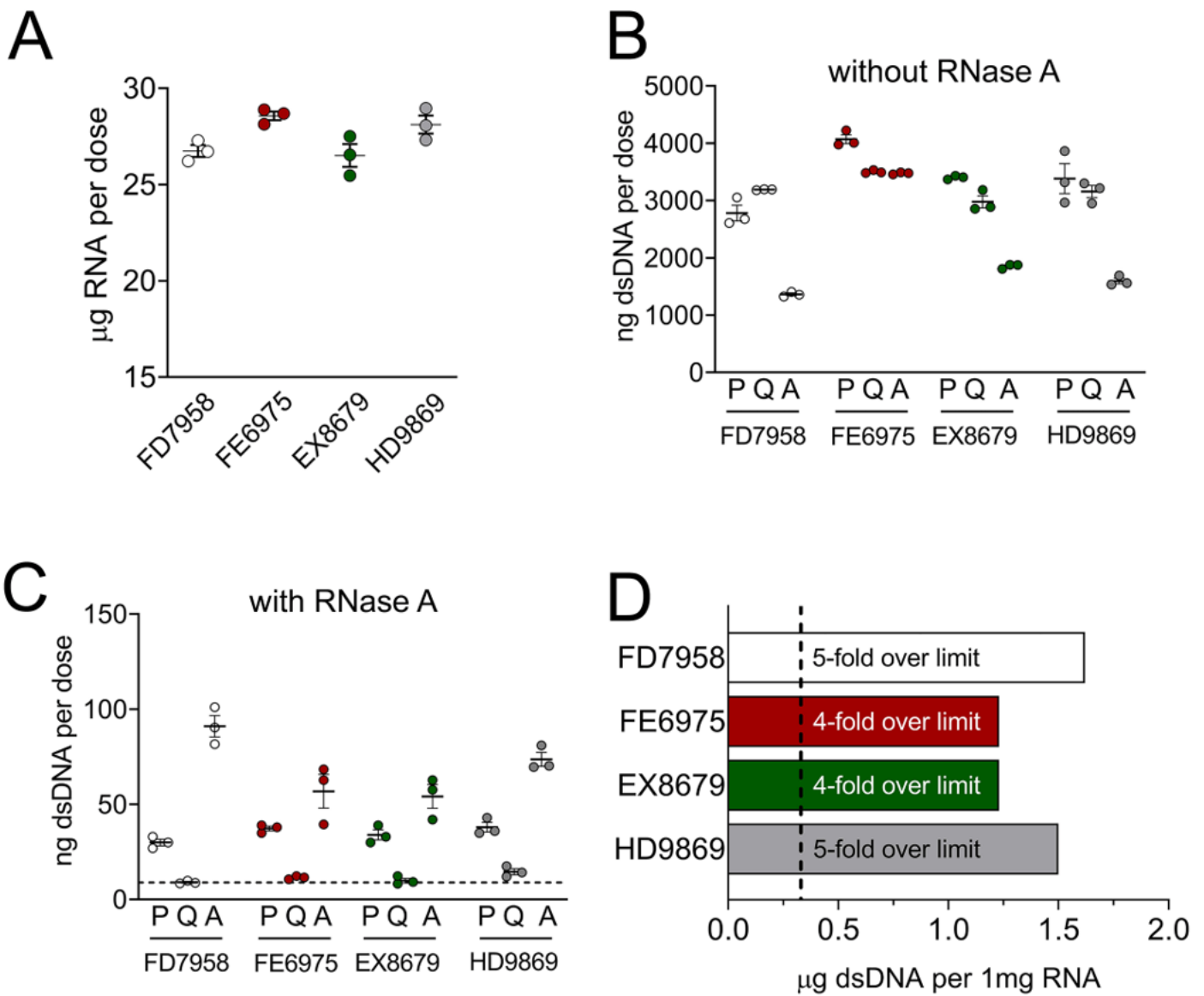


**Figure 2.**

RNA and DNA content of different BNT162b2 biologicals. A: Levels of modRNA per clinical dose were determined in vials by Qubit.  $n=3$ ,  $\text{mean} \pm \text{SEM}$ . B-C: Levels of double-stranded (ds) DNA per clinical dose in different vials measured by Picco Green (P), Qubit (Q) and AccuBlue (A) without RNase A (Figure B) and with RNase A (C) treatment. The dashed line shows the EMA limit of allowed dsDNA levels in biologicals.  $n=3$ ,  $\text{mean} \pm \text{SEM}$ . D: Ratio between the dsDNA and RNA content of the vials and the limit that was exceeded according to the EMA regulation of  $0.33\text{mg dsDNA per } 1\text{mg RNA}$  (dashed line). SEM, standard error of the mean.

### **Large Amounts Of DNA Are Found In The Tested RNA Vaccine Lots**

Due to reports on residual DNA of the BNT162b2 lots [27], all four lots used herein were analyzed with three different methods for possible residual DNA that could result from the manufacturing process using DNA plasmids and E. coli expression systems. Three DNA quantification systems Quant-iT PicoGreen dsDNA Assay (P), Qubit 1x dsDNA High Sensitivity Assay (Q), and AccuBlue dsDNA High Sensitivity Assay (A) were applied directly to the original vaccine solutions. Results are summarized in Figure 2B.

In a pre-test, we applied 1% Triton-X-100 in order to open the LNP and to quantify the whole amount of dsDNA (free and packed within LNP) present in the vials. As summarized in Table 3, the dsDNA content in the original untreated samples was clearly lower (factor 1.6-6.7 depending on the batch) when compared with the aliquots treated

with Triton-X-100. All following experiments have been performed with Triton-X-100 treatment.

	Without Triton X-100	With Triton X-100	
	ng $\pm$ SEM dsDNA per clinical dose	ng $\pm$ SEM dsDNA per clinical dose	Factor
<b>FD7958</b>	1514.00 $\pm$ 142.1	2446 $\pm$ 279.7	1.6
<b>FE6975</b>	962.90 $\pm$ 98.55	3683 $\pm$ 99.57	3.8
<b>EX8679</b>	410.00 $\pm$ 43.44	2745 $\pm$ 233.1	6.7
<b>HD9869</b>	577.80 $\pm$ 61.83	2712 $\pm$ 292.8	4.7

**Table 3.**

DNA levels in the indicated vials of BioNTech batches before RNase A treatment, without and with Triton-X-100 treatment. Factor represents the increase in DNA upon release of nucleic acids from the Triton-broken LNP. SEM, standard error of the mean.

A direct analysis of the contents of the vials diluted 1:10 with RNase-free buffered saline with 1% Triton-X-100 revealed high concentrations of double stranded (ds) DNA between 1326 – 4225 ng per clinical dose, with the AccuBlue method showing the lowest DNA concentrations in three lots and the same concentration as the Qubit method in the FE6975 lot. For three of the four lots tested (FE6976, EX8679, and HD9869), the Pico Green assay showed the highest DNA concentration, while for lot FD7958 the Qubit assay showed a slightly higher DNA concentration than the Pico Green assay. The internal variation within a lot and measurement method was minimal, which exclude any handling errors and confirmed the robustness of the results. This comparison of the three different analysis systems showed partly similar, partly larger variations in DNA concentration in the respective lots pointing to an important aspect when comparing results between different analysis methods.

To exclude the possibility that the kits used, contrary to their claim that they are dsDNA-specific, do partially detect RNA in the presence of high amounts of RNA, the same samples that were previously measured in Figure 2B were subsequently treated with RNase A (Table 4). Within 3 min, the DNA readings dropped dramatically and remained stable for the remaining 30 min of incubation suggesting that a) the intercalating dyes indeed do react with RNA and b) RNase treatment sufficiently deleted all interfering RNA with no remaining RNA being present in the samples at the end of the treatment. Again, there was only minimal variation within the triplicates analyzed independently. It is interesting to note that the measurement with AccuBlue from the untreated samples showed the lowest DNA level and with RNase-A treatment the highest content reflecting the lowest interaction with RNA of the three test systems used. It seems that AccuBlue shows the least cross talk with RNA when measuring DNA concentrations, which fits to the observation described by others [34]. From this data, it can be assumed that the DNA values obtained after RNase-A treatment represented the real DNA concentration in the vials without interfering RNA. This now “pure” residual DNA of the individual vials was between 32.71 ng and 43.38 ng per clinical dose (Figure 2C). This corresponds to 1.23  $\mu$ g – 1.62  $\mu$ g dsDNA per mg RNA and thus exceeds the upper DNA limit of the European Medicine Agency (EMA) by 4-5 times (Table 2; Figure 2D).

	Without RNase-A		With RNase-A		Factor
	$\mu\text{g} \pm \text{SEM}$ RNA per clinical dose	$\text{ng} \pm \text{SEM}$ dsDNA per clinical dose	$\text{ng} \pm \text{SEM}$ dsDNA per clinical dose	$\mu\text{g}$ dsDNA per mg RNA	
FD7958	$26.74 \pm 0.31$	$2446 \pm 279.7$	$43.38 \pm 12.42$	1.62	5
FE6975	$28.57 \pm 0.22$	$3683 \pm 99.57$	$35.25 \pm 7.06$	1.23	4
EX8679	$26.51 \pm 0.59$	$2745 \pm 233.1$	$32.71 \pm 6.69$	1.23	4
HD9869	$28.12 \pm 0.47$	$2712 \pm 292.8$	$42.09 \pm 8.69$	1.50	5

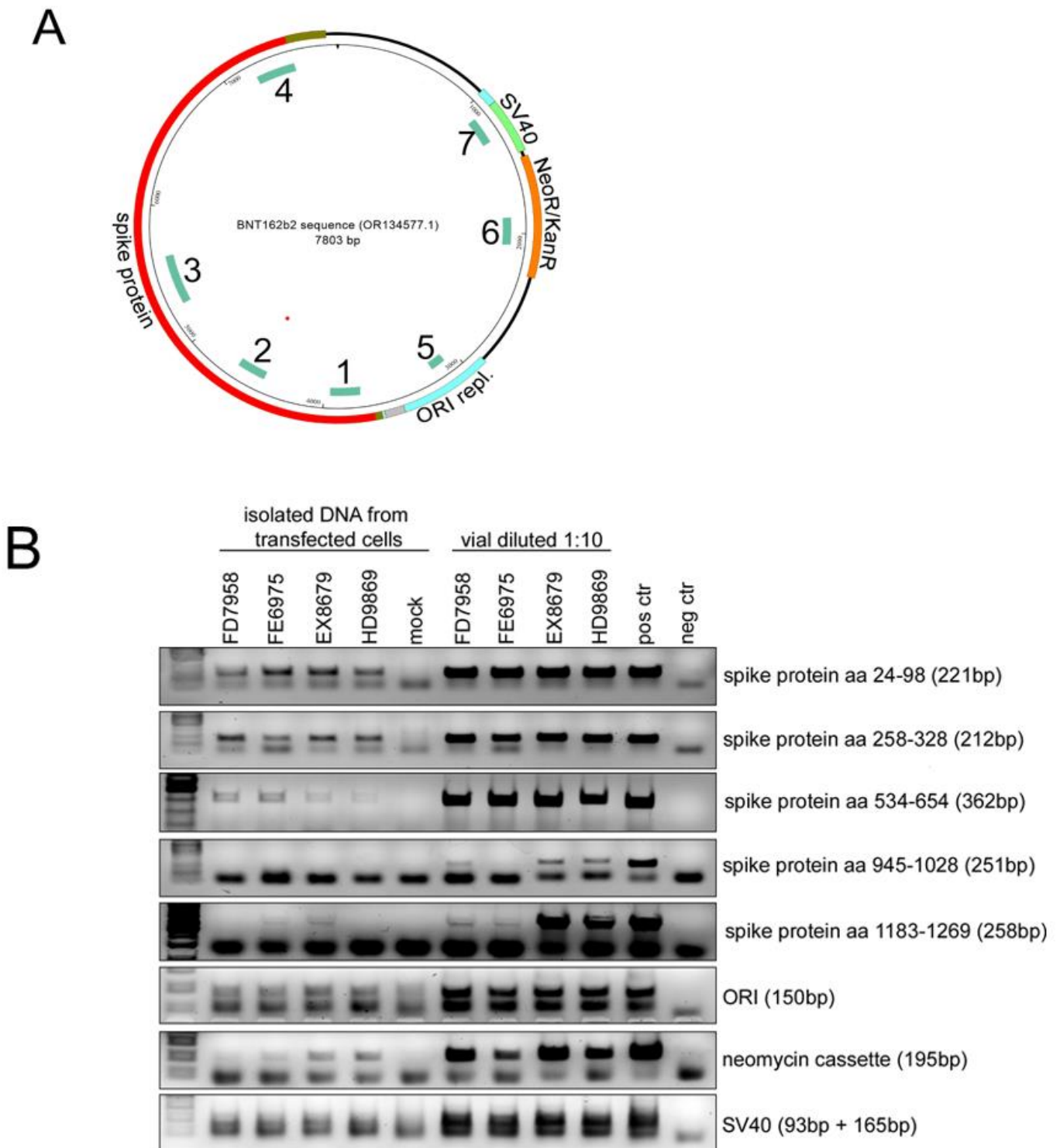
**Table 4.**

CRNA and DNA levels (following Triton-X-100 treatment) in the indicated vials of BioNTech lots before and after RNase A treatment. Factor represents the multiplier for exceeding the limit value in accordance with the EMA regulation of 0.33ug dsDNA per 1mg RNA. SEM, standard error of the mean.

***Residual DNA Contains Process-Related Plasmid Elements And Is Taken Up By The Cells***

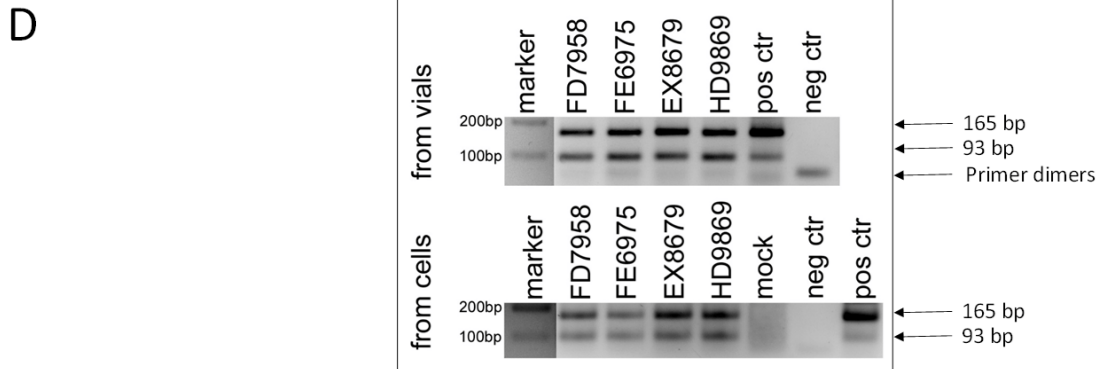
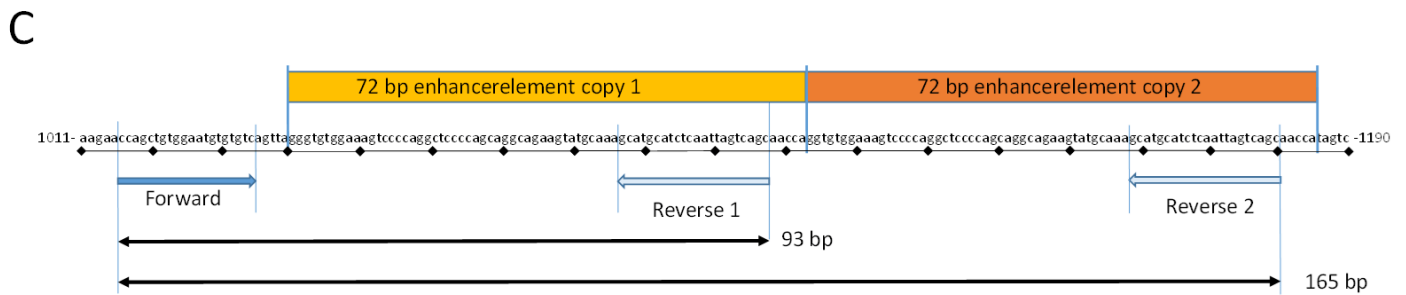
To determine whether the DNA found in the vials originates from the plasmid-DNA used for the mRNA production process, primer pairs were generated against sequences of various genes (SV40 promoter/enhancer, neomycin cassette, ORI replicon, and spike protein) representing the whole map of the plasmid (Figure 3A). A vial containing lot GH9715 was used as a positive control, as plasmid-DNA from this lot was already isolated and sequenced [21,22] and confirmed to refer to the plasmid sequence BNT162b2 (GenBank PP544445.1, GenBank PP544446.1, GenBank MQ287666.1 representing sequence 16 from patent WO2021214204) published by BioNTech. McKernan was able to prove that the identified DNA was indeed the plasmid DNA required for the mRNA production process. The positive control showed a DNA fragment of the correct size for all primer pairs (Figure 3B). The negative control (water) revealed no signal at all. Interestingly, all four vials tested at a dilution of 1:10 showed strong signals for all DNA fragments of the different genes.

To investigate whether HEK293 cells in our system were not only transfected with the vaccine RNA (resulting in the proven spike expression) but in addition with residual plasmid-DNA, DNA was isolated and purified from carefully washed and isolated transfected cells. As shown in Figure 3B, we were able to detect all PCR products of the correct size representing the investigated plasmid genes in the cells after transfection with all four lots. Consistent with the two copies of the 72 bp SV40 promoter/enhancer element interconnected in a cassette-like manner in the plasmid (Region bases 1041 – 1185 of GenBank PP544446; Figure 3C), the SV40 promoter/enhancer PCR resulted in two amplicons of the expected sizes (Figure 3D). These positive signals were even possible with only 1-10% of the amount of DNA normally used in the PCR reaction (Figure 3B).



**Figures 3A & 3B.**

Polymerase chain reaction (PCR) reveals residual DNA of the complete plasmid used in the modRNA production process. A: Schematic representation of the DNA plasmid used by BioNTech as a template for modRNA production. Specific sequences (SV40 promoter/enhancer; neomycin resistant cassette, ORI replicon, spike protein) are highlighted in color, as are the sequences used to detect these genes, which are numbered from 1 to 7. B: Visualized DNA fragments after PCR of the indicated sequences (Figure A, 1-7) show the detection of all genes from the DNA plasmid in the vials (right, diluted 1:10 before loading to the PCR) and in plasmid preparations from cells transfected with these biologicals (left). Mock stands for non-transfected cells as negative control for the left part and water as negative control for the right part. Lot GH9715 served as positive control.



### Figures 3C & 3D.

Polymerase chain reaction (PCR) reveals residual DNA of the complete plasmid used in the modRNA production process. C: Map of the SV40 promoter/enhancer region shows the two copies of the 72bp element that result in the two amplicons visible in the PCR due to two binding-sites of the reverse primer in combination with the single binding-site of the forward primer. D: Additional PCR for the SV40 promoter/enhancer (same PCR conditions as in Figure 3B except for a longer runtime) in order to better separate and visualize the two amplicons at 165 bp and 93 bp.

## Discussion

We analyzed the nucleic acid content of four BNT162b2 (Comirnaty) vials distributed in Germany and found that the RNA concentration fits with the manufacturer's specification of 30 µg per clinical dose demonstrating the accuracy of our analysis. In addition, we identified residual DNA including plasmid-DNA in amounts similar to that reported by McKernan et al. [21,22] for US-Pfizer lots. DNA concentrations in the vials analyzed in this study ranged from 32.7 to 43.4 ng per clinical dose after eliminating RNA via RNase digestion. This far exceeds the maximal upper limit of 10 ng per clinical dose, which the WHO has declared to be tolerable in injectable biologicals [35].

In order to allow the analysis of the total DNA content present in the vials, we performed Triton-X-100 treatment to open the LNP. Comparison of the untreated vaccine solutions with the Triton-X-100 treated paired aliquots exhibited a 1.6-fold to 6.7-fold increase of the DNA content, which probably reflects a high variability in the LNP packing of the DNA leftovers during the manufacturing process. Our results are in accordance with data from Raoult [36], who recently reported a clear increase of the DNA content after LNP opening in one Comirnaty batch. The amount of residual DNA, released from the LNP by treatment with Triton-X-100, analyzed in this study is less than that reported recently [27]. We suspect that this may be due to cross-interaction of RNA with intercalating dyes [37]. Indeed, when samples were treated with RNase, DNA concentrations were markedly reduced, albeit to levels that still remained manyfold above the limits that have been

deemed acceptable for naked DNA. In a recent preprint [38], product-related DNA impurities in BNT162b2 have been reported to coincide with the approved mRNA specifications. However, authors performed an additional ethanol precipitation step prior to Qubit analysis, which is known to inefficiently precipitate short DNA sequences representing the majority of reminiscent DNA after DNase digestion during the manufacturing process. This approach resulted in a high intra-batch variability of the calculated RNA amount in two Comirnaty batches. While our results (obtained without ethanol precipitation) showed an only low scattering between batches and an RNA content nearly identical and next to the 30 µg content specified per dose, the calculated RNA content by Kaiser et al. [38] was much lower with a maximum of 20 µg per dose. This suggests that they probably lost a considerable amount of nucleic acids during sample preparation. As is the case for the low resulting RNA concentration, also their DNA analysis resulted in far too low concentrations and do not represent the real residual DNA content when compared with the initial DNA concentration in the vials (free and packed in LNP) before the precipitation, washing, and resolution step losses.

Of note, official limit values for residual DNA in biologicals are defined for antibodies, attenuated vaccines, and protein solutions, but not for RNA injections and – even more important – for nucleic acids packaged in transfection reagents like lipid nanoparticles, which were used for the first time in the COVID-19 injections [39]. In fact, no scientific evidence exists that would permit a safety level of residual DNA to be defined in such injectables whatsoever.

Yet more concerning is the identification of gene sequences that disclose residuals of the BNT162b2 lots with plasmid-DNA that was employed as the expression system in the manufacturing process [9]. Originally, the presence of intact plasmids was demonstrated by McKernan and colleagues [21,22] in transformation experiments, whereby plasmid-encoded kanamycin resistance was conferred on to recipient *E. coli*. However, the complementary question of whether transfection of human cells might also occur has not yet been addressed. After transfection of cell cultures without any additional transfection reagents, plasmid-derived sequences like the kanamycin gene and SV40 promoter/enhancer could subsequently be re-isolated from transfected cells, suggesting that packaging into lipid nanoparticles and transfection into the cells had occurred, since free, unpackaged DNA would not be taken up by the cells. Cellular uptake is thus not followed by rapid degradation and disposal of plasmid-DNA. While further investigations need to clarify whether the residual plasmid-DNA also can serve as a template for the generation of functional proteins in the cell, our results leave no room for doubt that residual plasmid-DNA and fragments derived thereof that are contained in the RNA biologicals will enter myriads of cells in the human recipients. We could not demonstrate, whether some of the transfected cells contained the intact plasmids, however, the presence of the identified SV40 promoter/enhancer region is highly worrying regardless of the presence of the plasmid [23,40,41].

Our molecular analyses of the plasmid components confirmed data reported by McKernan and colleagues [21,22], namely the presence of a DNA sequence of the SV40 promoter/enhancer. This sequence was not declared in the plasmid map that BioNTech/Pfizer submitted in the approval procedure [42, page 24]. This finding is very surprising and raises the legitimate question: Why did BioNTech/Pfizer apply this totally unnecessary but highly dangerous element in their plasmids and use it as a template for

the production of modRNA? In our opinion, BioNTech/Pfizer must be held accountable for incorporating this highly dangerous element in their plasmids.

By design, the plasmids used by BioNTech and Pfizer are so-called shuttle vectors. They contain cloning sites and polyadenylation signals, as well as elements that are necessary for replication and translation in bacterial systems, like the T7 phage promoter, and in addition a promoter/enhancer element in order to permit transcription initiation in eukaryotic cells, which usually derives from viruses like CMV or SV40. One of the first shuttle vectors which served as a kind of prototype for the current BioNTech/Pfizer plasmid was established as early as 1988 [43]. A similar SV40 component containing mammalian expression vectors [Addgene: pcDNA3.1 SARS-CoV-2 S D614, however, without the bacterial components], were used already in 2020 for the analysis of spike protein functions in human cell lines [44].

According to the official generation process of the RNA coding for the spike protein, no eukaryotic promoter/enhancer is necessary, since the whole process-2 is performed in-vitro in the bacterial E. coli system. In addition, amongst available strong viral promoter/enhancer elements, like CMV, Bakulovirus, and RSV, the SV40 element is the most dangerous for the integrity of the target cells since long before the development of RNA biologicals, it was shown that the 72 bp SV40 promoter/enhancer fragment facilitates maximal transport of plasmid-DNA into the nucleus of transfected cells [23,41], a feature not found in CMV and RSV elements. Explicitly, one aspect should raise the alarm bell which is expressed by Dean et al. [23]: “The inclusion of this SV40 sequence in non-viral vectors may greatly increase their ability to be transported into the nucleus especially in non-dividing cells.” This transport of plasmids containing the SV40 promoter/enhancer element into the nucleus was found for a broad variety of cell types tested [45] leading to the promotion of the SV40 promoter/enhancer element for highly effective gene therapy approaches. The detection of the SV40 promoter/enhancer sequences begs the question what intention the manufacturers had when selecting an expression system containing this mammalian cell active element instead of selecting a pure prokaryotic expression system for the manufacturing process.

Finally, we demonstrate that transfected cells are able to produce and secrete spike proteins. We did not use any other transfection-enhancing substances in any of the transfections. This enabled us to analyze the direct gene transfer of the pure substance from the lipid nanoparticles as a “transfection reagent” into the host cells simulating the situation in the vaccinated individuals. It is known that an additional administration of transfection enhancers, such as apolipoprotein E3 (ApoE3), which binds to the cholesterol of the lipid envelope of the LNP and thus facilitates the uptake of the LNP into the cells via ApoE3 receptors, would have led to a higher transfection efficiency. The transfection efficiency can also be increased by changing the target cell line or increasing the administration of LNP. Our measured values of intracellular and extracellular spike concentrations therefore only refer to the HEK293 cells under the specified parameters, which are described in detail in the methods section. After transfection, our cells exhibited large intracellular vesicles representing a clear feature of cell health impairment after uptake of the modRNA containing LNP. The envelope of the latter consists of four lipid components. In particular, the group of cationic (ionizable) lipids is well-known for its toxic and pro-inflammatory effect on cells both in-vitro and in-vivo [46]. It is currently unknown how many and which cell types in the body are affected, but it has been reported that the LNP spread throughout the body and the modRNA is found in all organs examined [9].

We discerned that the production of spike proteins lasts for many days. After one week, even more spike proteins are present in the cells than after 24 hours, although the highest modRNA level is expected after 24 hours, before it is degraded. The amount of spike proteins produced varied between lots, but the progression over time was identical for all, with a peak on day 5 after transfection. We also showed that the level of production is related to the amount of injected modRNA, as lot HD9869 reveals a significantly lower spike protein level than the other three lots. This was due to the fact that HD9869 is a bivalent vaccine consisting of two different modRNAs for two different spike protein variants, namely the Wuhan variant and the Omicron variant. As the ELISA applied in this study detects only the Wuhan variant, the spike proteins produced by the Omicron variant are not detectable and we obtain lower values than for the three monovalent vaccines with only the Wuhan variant.

Using mass spectrometry, we were able to demonstrate that the spike proteins are almost exclusively released into the medium via exosomes. In case of an in-vivo situation, this would mean that the spike proteins are transported within exosomes to other tissues and organs via the blood stream and, consequently, taken up by the target cells. In fact, it has already been reported that spike proteins can be found in exosomes of vaccinated individuals [10]. The functions of exosomes are manifold. They mainly serve as a communication platform between cells of the same tissue and between cells of different organs. The exosomes are easily taken up by the target cells through various mechanisms and the content thus enters the target cell and induces a structural and functional response [47]. In the case of BNT162b2, it can be assumed that spike proteins can be transferred and taken up from one tissue to the next in this way regardless of the presence of LNP or modRNA. Whether the target cells are damaged by the uptake of spike protein-containing exosomes has not yet been investigated. However, this potent transfection ability raises alarm clocks in light of the background of the co-transfected residual DNA and especially the SV40 promoter/enhancer elements of the primary material, the plasmid. In preliminary experiments, another lot of BNT162b2 was able to transfect ovarian cancer cells and here, parts of the transfected nucleic acid material were indeed found by whole genome sequencing to be integrated into chromosomes 9 and 12 of the cells [48].

The sequence of the modRNA shows that the leader sequence for the translation of the spike protein into the lumen of the endoplasmic reticulum and the sequence for the membrane anchor were not removed from the modRNA. As a consequence, the produced spike proteins are predominantly expressed on the cell surface. According to BioNTech, the modRNA is translated in the cytosol [49]. This would mean that the spike proteins remain inside the cells and are not presented as full-length proteins on the cell surface. However, this contradicts the function of a leader and an anchor sequence within RNA in other membrane proteins. The possibility of shedding of the spike proteins was also not considered by BioNTech [49].

### ***Limitation Of The Study and Variability Of The Data***

We used technical and biological replicates (where appropriate) to reproduce our results and determine variability. As the variability for each experiment was small within a group, we can rule out technical artifacts. We only had access to a few lots, but we considered them sufficient to demonstrate the fundamental problem of residual DNA and cell transfection by “RNA vaccines.” When experiments were carried out (2023), the expiration date of the three monovalent vaccine lots specified by the manufacturer had already

passed. Due to the fact that the vials were consistently stored unopened at -80 °C and that the expiration date was extended officially several times by the German Paul Ehrlich Institute (PEI) [50: 10. Sept 2021 from 6 to 9 months; 51: 24. March / 4. April 2022 from 9 to 12 months; 52: 2. Dec 2022 from 12 to 18 months], we do not expect any negative effects on our results. We cannot rule out that the vaccines also contain and transfect stable double-stranded RNA (dsRNA) and RNA:DNA hybrids in parallel to the single-stranded modRNA and the vector-based DNA. We are also unable to fully map the toxicity of LNP on different cell types. We used a relatively robust human embryonic kidney cell line for our experiments that is immortalized and can therefore withstand toxic substances up to a certain level. Further studies are necessary to test, for example primary cell cultures such as a primary neuronal cells or immune cells, which would react much more sensitively to LNP. Since it is known that LNP are distributed throughout the body and thus probably affect all cell types, further in vitro studies on toxicity, expression behavior, and proteome analysis must be carried out.

## Conclusion

---

We demonstrated that transfection of the human cell line HEK293 with four different BNT162b2 lots results in the production of spike proteins over several days, which are released into the cell supernatant via exosomes. We detected residual plasmid-DNA in all vials at concentrations far exceeding the allowed EMA limit of 0.33 ng dsDNA per 1 mg RNA. We identified all plasmid genes as well as the two copies of the SV40 promoter/enhancer element. The DNA was shown to enter and persist in the cells.

Already before the start of the governmental vaccination campaign, physicians and scientists pointed out that serious adverse events would be triggered by the gene-based agents. In the meantime, the spectrum of adverse side events has become so multifaceted that the term “spikeopathy” has been created to denote the new disease complex [53]. The eternal dangers of all RNA biologicals are 4-fold: First, modRNA encoding any foreign protein will trigger detrimental autoimmune reactions [54]. Second, the lipid nanoparticles are themselves highly toxic [55]. Third, residual plasmid-DNA and reverse transcribed mRNA will genetically modify cells. Fourth, replacement of uridine in natural mRNA by N1-methyl-pseudouridine in synthetic modRNA causes +1 ribosomal frameshifting resulting in haphazard production of utterly alien proteins [56].

Our results confirm and extend published reports and raise grave concerns regarding the safety of the BNT162b2 vaccine. We call for an immediate halt of all RNA-based biologicals until these concerns are scientifically addressed and convincingly dispelled.

## Acknowledgements

---

We thank the Proteomics Core Facility of the Amsterdam UMC in The Netherlands for mass spectrometry support and Maarten Fornerod for analyzing the mass spectrometry data to determine the abundance of plasmid and alternative ORF peptides.

---

## Author Contributions

Conceptualization, U.K., V.S. and K.S.; methodology, U.K and V.S.; software, V.S.; validation, U.K. and V.S.; formal analysis, U.K., V.S. and K.S.; investigation, U.K. and V.S.; resources, U.K. and V.S.; data curation, U.K. and V.S.; writing—original draft preparation, U.K., V.S. and K.S.; writing—review and editing, U.K., V.S. and K.S.; visualization, U.K. and V.S.; supervision, U.K., V.S. and K.S.; project administration, V.S. and K.S.; All authors have read and agreed to the published version of the manuscript.

## Funding

This research received no external funding.

## Conflicts of Interest

The authors declare no conflicts of interest.

## References

---

1

Winch, G.M., Cao, D., Maytorena-Sanchez, E., Pinto, J., Sergeeva, N., Zhang, S. Operation Warp Speed: Projects responding to the COVID-19 pandemic. *Project Leadership and Society*. 2:100019. 2021. <https://doi.org/10.1016/j.plas.2021.100019>

2

Operation Warp Speed. 2021. Available online: <https://www.gao.gov/products/gao-21-319> (accessed on 25.06.2024)

3

Türeci, Ö., Sahin, U. *Projekt Lightspeed* (German). 2021. ISBN10 3498002775.

4

Project Lightspeed. 2020. Available online: [https://www.pei.de/SharedDocs/Downloads/EN/newsroom-en/dossiers/ppt-erste-studie-sars-cov-2-impfstoff-en.pdf?\\_\\_blob=publicationFile&v=2](https://www.pei.de/SharedDocs/Downloads/EN/newsroom-en/dossiers/ppt-erste-studie-sars-cov-2-impfstoff-en.pdf?__blob=publicationFile&v=2) (accessed on 25.06.2024)

5

France24. 2020. Available online: <https://www.pfizer.com/science/innovation/mrna-technology> (accessed on 25.06.2024)

6

Webpage BioNTech. <https://www.biontech.com/int/en/home/pipeline-and-products/platforms/our-mrna-platforms.html>

7

Webpage Pfizer. <https://www.pfizer.com/science/innovation/mrna-technology>

8

Shot of a lifetime. Available

online: [https://www.pfizer.com/news/articles/shot\\_of\\_a\\_lifetime\\_how\\_pfizer\\_and\\_biontech\\_developed\\_and\\_manufactured\\_a\\_covid\\_19\\_vaccine\\_in\\_record\\_time](https://www.pfizer.com/news/articles/shot_of_a_lifetime_how_pfizer_and_biontech_developed_and_manufactured_a_covid_19_vaccine_in_record_time) (accessed on 24.06.2024)

9

EMA Assessment Report. 2021. Available

online: [https://www.ema.europa.eu/en/documents/assessment-report/comirnaty-epar-public-assessment-report\\_en.pdf](https://www.ema.europa.eu/en/documents/assessment-report/comirnaty-epar-public-assessment-report_en.pdf) (accessed on 25.06.2024)

10

Bansal, S., Perincheri, S., Fleming, T., Poulson, C., Tiffany, B., Bremner, R.M., Mohanakumar, T. Cutting Edge: Circulating exosomes with COVID spike protein are induced by BNT162b2 (Pfizer-BioNTech) vaccination prior to development of antibodies: A novel mechanism for immune activation by mRNA vaccines. *Journal of Immunology*. 207:2405-2410. 2021. <https://doi.org/10.4049/jimmunol.2100637>

11

Mörz, M. A Case Report: Multifocal Necrotizing Encephalitis and Myocarditis after BNT162b2 mRNA Vaccination against COVID-19. *Vaccines*. 10:1651. 2022. <https://doi.org/10.3390/vaccines10101651>

12

Hanna, N., Lin, X., Thomas, K., Vintzileos, A., Chavez, M., Palaia, T., Ragolia, L., Verma, S., Khullar, P., Hanna, I. Underestimation of SARS-CoV-2 infection in placental samples. *American Journal of Obstetrics and Gynecology*. 225:572-575.e1. 2021. <https://doi.org/10.1016/j.ajog.2021.07.010>

13

Dhuli, K., Medori, M.C., Micheletti, C., Donato, K., Fioretti, F., Calzoni, A., Praderio, A., De Angelis, M.G., Arabia, G., Cristoni, S., Nodari, S., Bertelli, M. Presence of viral spike protein and vaccinal spike protein in the blood serum of patients with long-COVID syndrome. *European Review for Medical and Pharmacological Sciences*. 27 (Suppl. 6):13-19. 2023. [https://doi.org/10.26355/eurrev\\_202312\\_34685](https://doi.org/10.26355/eurrev_202312_34685)

14

Sahin, U., Karikó, K., Türeci, Ö. mRNA-based therapeutics—developing a new class of drugs. *Nature Reviews Drug Discovery*. 13:759-780. 2014. <https://doi.org/10.1038/nrd4278>

15

Kariko, K., Buckstein, M., Ni, H., Weissman, D. Suppression of RNA recognition by Toll-like receptors: the impact of nucleoside modification and the evolutionary origin of RNA. *Immunity*. 23:165-175. 2005. <https://doi.org/10.1016/j.immuni.2005.06.008>

16

Granados-Riveron, J.T., Aquino-Jarquín, G. Engineering of the current nucleoside-modified mRNA-LNP vaccines against SARS-CoV-2. *Biomedicine and Pharmacotherapy*. 142. 2021. <https://doi.org/10.1016/j.biopha.2021.111953>

17

Zhang, L., Richards, A., Barrasa, M.I., Jaenisch, R. Reverse-transcribed SARS-CoV-2 RNA can integrate into the genome of cultured human cells and can be expressed in patient-derived tissues. *Proceedings of the National Academy of Sciences*. 118:e2105968118. 2021. <https://doi.org/10.1073/pnas.2105968118>

18

Alden, M., Olofsson Falla, F., Yang, D., Barghouth, M., Luan, C., Rasmussen, M., De Marinis, Y. Intra-cellular reverse transcription of Pfizer BioNTech COVID-19 mRNA vaccine BNT162b2 in vitro in human liver cell line. *Current Issues in Molecular Biology*. 44:1115-1126. 2022. <https://doi.org/10.3390/cimb44030073>

19

Sutton, D.H., Conn, G.L., Brown, T., Lane, A.N. The dependence of DNase I activity on the conformation of oligodeoxynucleotides. *Biochemical Journal*. 321:481-486. 1997. <https://doi.org/10.1042/bj3210481>

20

Webpage Thermofisher. <https://www.thermofisher.com/de/de/home/references/ambion-tech-support/nuclease-enzymes/general-articles/dnase-i-demystified.html>

21

McKernan, K. Pfizer and Moderna bivalent vaccines contain 20-35% expression vector and are transformation competent in *E. coli*. 2023. <https://anandamide.substack.com/p/pfizer-and-moderna-bivalent-vaccines>

22

McKernan, K., Helbert, Y., Kane, L.T., McLaughlin, S. Sequencing of bivalent Moderna and Pfizer mRNA vaccines reveals nanogram to microgram quantities of expression vector dsDNA per dose. *OSF Preprints*. 2023. <https://doi.org/10.31219/osf.io/b9t7m>

23

Dean, D.A., Dean, B.S., Muller, S., Smith, L.C. Sequence requirements for plasmid nuclear import. *Experimental Cell Research*. 253:713-22. 1999. <https://doi.org/10.1006/excr.1999.4716>

24

Sequencing the Pfizer monovalent mRNA vaccines also reveals dual copy 72-bp SV40 Promoter. 2023. <https://anandamide.substack.com/p/sequencing-the-pfizer-monovalent>

25

25. Vaccine targeted qPCR of Cancer Cell Lines treated with BNT162b2. 2024. <https://anandamide.substack.com/p/vaccine-targeted-qpcr-of-cancer-cell>

26

Speicher, D.J., Rose, J., Gutsch, L.M., Wiseman, D.M., McKernan, K. DNA fragments detected in monovalent and bivalent Pfizer/BioNTech and Moderna modRNA COVID-19 vaccines from Ontario, Canada: Exploratory dose response relationship with serious adverse events. OSF Preprints. 2023 <https://doi.org/10.31219/osf.io/mjc97>

27

König, B., Kirchner, J.O. Methodological considerations regarding the quantification of DNA impurities in the COVID-19 mRNA vaccine Comirnaty. *Methods and Protocols*. 7:41. 2024. <https://doi.org/10.3390/mps7030041>

28

Ghosh, A.A., Davey, M., Chute, I.C., Griffiths, S.G., Lewis, S., Chacko, S., Barnett, D., Crapoulet, N., Fournier, S., Joy, A., Caissie, M.C., Ferguson, A.D., Daigle, M., Meli, M.V., Lewis, S.M., Ouellette, R.J. Rapid isolation of extracellular vesicles from cell culture and biological fluids using a synthetic peptide with specific affinity for heat shock proteins. *PLoS One*. e110443. 2014. <https://doi.org/10.1371/journal.pone.0110443>

29

Knol, J.C., de Reus, I., Schelfhorst, T., Beekhof, R., De Wit, M., Piersma, S.R., Pham, T.V., Smit, E.F., Verheul, H.M.W., Jiménez, C.R. Peptide-mediated 'miniprep' isolation of extracellular vesicles is suitable for high-throughput proteomics. *European Proteomics Association Open Proteomics*. 11:11–15. 2016 <https://doi.org/10.1016/j.euprot.2016.02.001>

30

Piersma, S.R., Warmoes, M.O., De Wit, M., De Reus, I., Knol, J.C., Jiménez, C.R. Whole gel processing procedure for GeLC- MS/MS based proteomics. *Proteome Science*. 11:17. 2013. <https://doi.org/10.1186/1477-5956-11-17>

31

Garcia de Durango, C.R., Monteiro, M.N., Bijnsdorp, I.V., Pham, T.V., De Wit, M., Piersma, S.R., Knol, J.C., Pérez-Gordo, M., Fijneman, R.J.A., Vidal-Vanaclocha, F., Jimenez, C.R. Lipopolysaccharide-regulated secretion of soluble and vesicle-based proteins from a panel of colorectal cancer cell lines. *Proteomics Clinical Applications*. 15:1900119. 2021. <https://doi.org/10.1002/prca.201900119>

32

Liu, H., Sadygov, R.G., Yates, J.R. A model for random sampling and estimation of relative protein abundance in shotgun proteomics. *Analytical Chemistry*. 76:4193–4201. 2004. <https://doi.org/10.1021/ac0498563>

33

Kim, T.K., Eberwine, J.H. Mammalian cell transfection: the present and the future. *Analytical and Bioanalytical Chemistry*. 397:3173-3178. 2010. <https://doi.org/10.1007/s00216-010-3821-6>

34

Bruijns, B.B., Tiggelaar, R.M., Gardeniers, J.G.E. Fluorescent cyanine dyes for the quantification of low amounts of dsDNA. *Analytical Biochemistry*. 511:74-79. 2016. <https://doi.org/10.1016/j.ab.2016.07.022>

35

WHO Meeting Report. Study group on cell substrates for production of biologicals. 1–30. 2007. Available online: [https://cdn.who.int/media/docs/default-source/biologicals/cell-substrates/cells.final.mtgrep.ik.26\\_sep\\_07.pdf](https://cdn.who.int/media/docs/default-source/biologicals/cell-substrates/cells.final.mtgrep.ik.26_sep_07.pdf) (accessed on 25.06.2024)

36

Raoult, D. Confirmation of the presence of vaccine DNA in the Pfizer anti-COVID-19 vaccine. Preprint 2024. <https://hal.science/hal-04778576v1>

37

Jones, L.J., Yue, S.T., Cheung, C.Y., Singer, V.L. RNA quantitation by fluorescence-based solution assay: RiboGreen reagent characterization. *Analytical Biochemistry*. 265:368-374. 1998. <https://doi.org/10.1006/abio.1998.2914>

38

Kaiser, S.M., Kaiser, S.R., Reis, J., Marschalek, R. Quantification of objective concentrations of DNA impurities in mRNA vaccines. Preprint 2024. <https://ssrn.com/abstract=5009375> <http://dx.doi.org/10.2139/ssrn.5009375>

39

Yang, H. Establishing acceptable limits of residual DNA. *Journal of Pharmaceutical Science and Technology*. 67:155-163. 2013. <https://doi.org/10.5731/pdaipst.2013.00910>

40

Graessmann, M., Menne, J., Liebler, M., Graeber, I., Graessmann, A. Helper activity for gene expression, a novel function of the SV40 enhancer. *Nucleic Acids Research*. 17:6603-6612. 1989. <https://doi.org/10.1093/nar/17.16.6603>

41

Young, J.L., Benoit, J.N., Dean, D.A. Effect of a DNA nuclear targeting sequence on gene transfer and expression of plasmids in the intact vasculature. *Gene Therapy* 10:1465-1470. 2003. <https://doi.org/10.1038/sj.gt.3302021>

42

Rapporteur Rolling Review. 2020. Available online: <https://factreview.gr/wp-content/uploads/2023/07/Rolling-Review-Report-Quality-COVID-19-mRNA-Vaccine-BioNTech.pdf> (accessed on 24.06.2024)

43

Mongkolsuk, S. Novel eukaryotic expression vectors which permit single-stranded replication in *Escherichia coli* and in vitro translational analysis of cloned genes. *Gene*. 70:313-319. 1988. [https://doi.org/10.1016/0378-1119\(88\)90203-x](https://doi.org/10.1016/0378-1119(88)90203-x)

44

Yurkovetskiy, L., Wang, X., Pascal, K.E., Tomkins-Tinch, C., Nyalile, T.P., Wang, Y., Baum, A., Diehl, W.E., Dauphin, A., Carbone, C., Veinotte, K., Egri, S.B., Schaffner, S.F., Lemieux, J.E., Munro, J.B., Rafique, A., Barve, A., Sabeti, P.C., Kyratsous, C.A., Dudkina, N.V., Shen, K., Luban, J. Structural and functional analysis of the D614G SARS-CoV-2 spike protein variant. *Cell*. 183:739-751.E8. 2020. <https://doi.org/10.1016/j.cell.2020.09.032>

45

Vacik, J., Dean, B.S., Zimmer, W.E., Dean, D.A. Cell-specific nuclear import of plasmid DNA. *Gene Therapy*. 6:1006-1014. 1999. <https://doi.org/10.1038/sj.gt.3300924>

46

\Ndeupen, S., Qin, Z., Jacobsen, S., Bouteau, A., Estanbouli, H., Igyártó, B.Z. The mRNA-LNP platform's lipid nanoparticle component used in preclinical vaccine studies is highly inflammatory. *iScience*. 24:103479. 2021. <https://doi.org/10.1016/j.isci.2021.103479>

47

Jadli, A.S., Ballasy, N., Edalat, P., Patel, V.B. Inside(sight) of tiny communicator: exosome biogenesis, secretion, and uptake. *Molecular and Cellular Biochemistry*. 467:77-94. 2020. <https://doi.org/10.1007/s11010-020-03703-z>

48

McKernan, K. Plasmid DNA replication in BNT162b2 vaccinated cell lines. 2024. <https://anandamide.substack.com/p/plasmid-dna-replication-in-bnt162b2>

49

MHRA. Public Assessment Report, Authorisation for Temporary Supply, COVID-19 mRNA Vaccine BNT162b2 (BNT162b2 RNA) concentrate for solution for injection. 2021. Available

online: [https://assets.publishing.service.gov.uk/media/63529601e90e07768265c115/COVID-19\\_mRNA\\_Vaccine\\_BNT162b2\\_UKPAR\\_PFIZER\\_BIONTECH\\_ext\\_of\\_indication\\_11.6.2021.pdf](https://assets.publishing.service.gov.uk/media/63529601e90e07768265c115/COVID-19_mRNA_Vaccine_BNT162b2_UKPAR_PFIZER_BIONTECH_ext_of_indication_11.6.2021.pdf))

50

Paul-Ehrlich Institute. <https://www.pei.de/EN/newsroom/hp-news/2021/211004-comirnaty-vaccine-shelf-life-extended.html>

51

Paul-Ehrlich Institute. <https://www.pei.de/EN/newsroom/hp-news/2022/220421-comirnaty-shelf-life-extended-to-12-months.html>

52

Paul-Ehrlich Institute. <https://www.pei.de/EN/newsroom/hp-news/2022/221230-comirnaty-shelf-life-extended.html>

53

Parry, P.I., Lefringhausen, A., Turni, C., Neil, C.J., Cosford, R., Hudson, N.J., Gillespie, J. 'Spikeopathy': COVID-19 Spike Protein Is Pathogenic, from Both Virus and Vaccine mRNA. *Biomedicines*. 11:2287. 2023. <https://doi.org/10.3390/biomedicines11082287>

54

Polykretis, P., Donzelli, A., Lindsay, J.C., Wiseman, D., Kyriakopoulos, A.M., Mörz, M., Bellavite, P., Fukushima, M., Seneff, S., McCullough, P.A. Autoimmune inflammatory reactions triggered by the COVID-19 genetic vaccines in terminally differentiated tissues. *Autoimmunity*. 56:1. 2023. <https://doi.org/10.1080/08916934.2023.2259123>

55

Segalla, G. Chemical-physical criticality and toxicological potential of lipid nanomaterials contained in a COVID-19 mRNA vaccine. *International Journal of Vaccine Theory Practice and Research*. 3:787-817. 2023. <https://doi.org/10.56098/ijvtpr.v3i1.68>

56

Mulroney, T.E., Pöyry, T., Yam-Puc, J.C., Rust, M., Harvey, R.F., Kalmar, L., Horner, E., Booth, L., Ferreira, A.P., Stoneley, M., Sawarkar, R., Mentzer, A.J., Lilley, K.S., Smales, C.M., von der Haar, T., Turtle, L., Dunachie, S., Klenerman, P., Thaventhiran, J.E.D., Willis, A.E. N1-methylpseudouridylation of mRNA causes +1 ribosomal frameshifting. *Nature*. 625:189–194. 2024 <https://doi.org/10.1038/s41586-023-06800-3>

